

Antigenic stimulation by BCG vaccine as an *in vivo* driving force for SIV replication and dissemination

RÉMI CHEYNIER¹, SOPHIE GRATTON¹, MATILDA HALLORAN², INGRID STAHRER^{1,3},
NORMAN L. LETVIN² & SIMON WAIN-HOBSON¹

¹Unité de Rétrovirologie Moléculaire, Institut Pasteur, 28 Rue du Dr. Roux, 75724 Paris cedex 15

²Harvard Medical School, Division of Viral Pathogenesis, Beth Israel Deaconess Medical Center,
330 Brookline Avenue, Boston MA 02215

³Present address: University Hospital Eppendorf, Dept. Immunology, Martinistr. 52, D-20246 Hamburg
R.C. and S. G. contributed equally to this work

The impact of antigenic stimulation on the dynamics of simian immunodeficiency virus (SIV) replication was studied following repeated intravenous BCG inoculation of a SIV infected macaque. At the site of a delayed type hypersensitivity reaction to purified protein derivative of *M. tuberculosis*, a distinctive SIV variant was noted, probably as a result of the infiltration of activated antigen-specific T cell clones as opposed to infection by blood borne virus *in situ*. The dynamics of SIV quasi-species in peripheral blood suggests sequential waves of viral replication, illustrating the role of antigenic stimulation as a driving force in viral dissemination and pathogenesis.

The cellular arm of the antigen specific immune system not only provides essential help for the co-ordination of immune responses to microbes and neo-antigens, but also identifies and eliminates infected cells. These functions are carried out by CD4 and CD8 T cells respectively. Human immunodeficiency virus (HIV) is produced at the heart of lymphoid structures whose purpose is the generation of antigen specific immune responses. Infection is strongly focused on CD4 T cells, although antigen presenting cells such as macrophages and dendritic cells may also support HIV replication *in vivo*, albeit at lower frequencies^{1,2}.

In vitro, replication of HIV in T lymphocytes is linked to cellular activation. Latently infected T lymphocytes can be induced to produce HIV after stimulation by mitogens, antigens or in a mixed lymphocyte reaction. Although infection of quiescent T lymphocytes can lead to partial reverse transcription, productive infection may be achieved only upon subsequent T cell activation³. The adaptation of HIV to activated CD4 T cells is reflected in the structure of the U3 region of the LTR which encodes many recognition sites for activation-dependent transcription factors, such as NF- κ B and NFAT-1 (for review see ref. 4). Other features of the biology of HIV, for example nuclear transport and integration, also reveal this link. *In vivo*, vaccination and microbial infections result in a transient increase of plasma viremia with a return to base line within a matter of weeks⁵⁻¹¹. Within splenic white pulps, the finding of viral founder effects as revealed by the sequence complexity of PCR amplified HIV DNA was attributed to the local recruitment and activation of antigen-specific T cell clones bearing HIV proviruses¹².

An important model of AIDS pathogenesis open to experimentation is that of SIV infection of macaques where events in the lymphoid organs closely parallel those in humans¹³. Ongoing SIV sequence variation is a marker for viral replication¹⁴⁻¹⁶ and, depending on the region studied, can be used to estimate the number of rounds of replication between sequences. With this in mind, the present study was designed to analyze the impact of BCG inoculation on SIV distribution in immunocompetent structures and peripheral blood.

BCG inoculation protocol

Three rhesus macaques (*Macacca mulatta*, Mm246, Mm247 and Mm250) infected with the SIV_{mac251} strain were inoculated intravenously three times with sonicated live BCG at 18, 61 and 64 weeks post-SIV infection, the time points being referred to as BCG1, BCG2 and BCG3 respectively (Fig. 1). Coincident with BCG3, a skin test was performed on the right eyelid of the animals to test their reactivity to PPD (purified protein derivative of *M. tuberculosis*). Peripheral blood samples were taken at numerous time points before and after BCG inoculations enabling analyses of T-cell repertoire and SIV quasispecies fluctuations in peripheral blood mononuclear cells (PBMC) (Fig. 1). Two days after BCG3, the animals were killed and lymphoid organs (spleen, axillary, maxillary and inguinal lymph nodes) were collected. Skin patches from the delayed type hypersensitivity (DTH) reaction site (right eyelid) and normal skin (left eyelid) were also sampled.

DTH reactions are mediated mainly by antigen-specific CD4+ T cells and macrophages infiltrating the test site together with other inflammatory cells¹⁷. A strong DTH response to PPD (> 6 mm) was observed for Mm247, while Mm246 showed no response (in keeping with the variability of BCG responses in macaques¹⁸) and was not studied further. Mm250 unfortunately died during anaesthesia. As even very weak antibody titers to PPD can usually be detected in sera from vaccinated individuals^{19,20}, sera from Mm247 were tested for BCG-specific antibodies in an ELISA. Reactivity was detected 21 days after BCG1 and sustained thereafter. Successive boosts did not increase the plasma antibody titers (data not shown).

T cell repertoire

To help define the T cell mediated response, analysis of the rearranged T cell receptor (TCR) V β chains of the T cells infiltrating the DTH site was performed by PCR amplification in a manner analogous to that previously described for the human TCRBV¹². In this type of analysis, each T cell clone is defined by a peak at

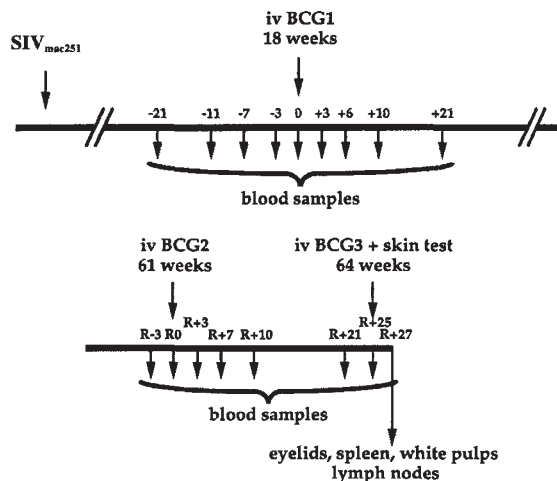


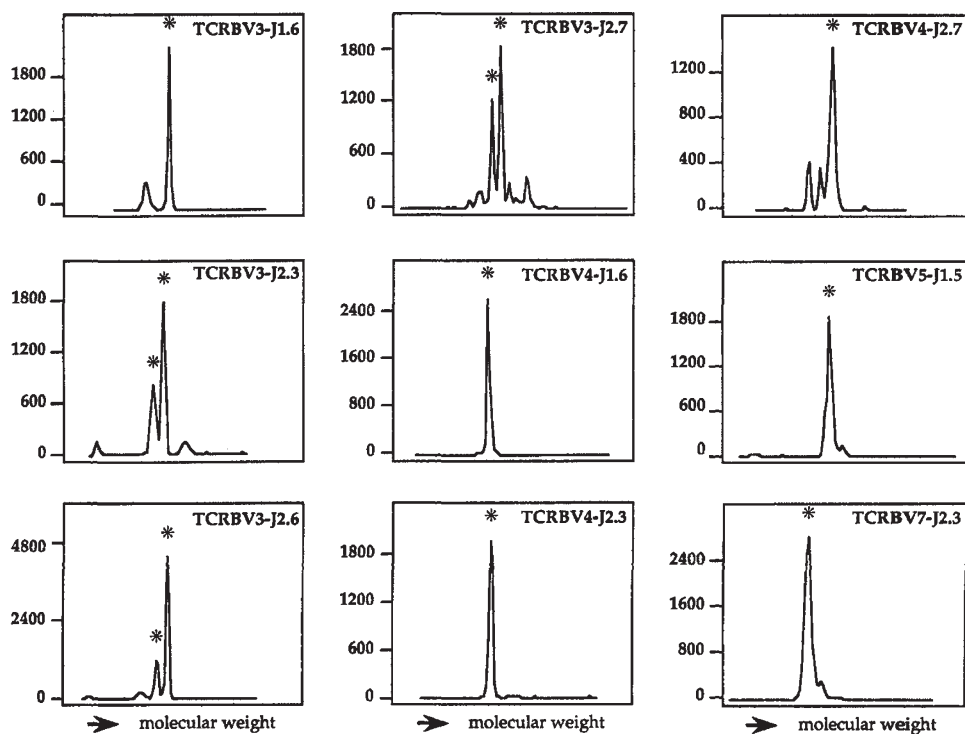
Fig. 1 BCG inoculation protocol.

specific molecular weight related to the length of the TCRBV CDR3. Peak areas are proportional to the size of the clonal population. Generally, a discrete peak represents a single clone as confirmed by sequencing (ref. 12 and data not shown). Given the patterns of TCRBV/BJ usage^{21,22}, approximately 80% of the repertoire was covered.

Twenty-one major and 91 minor peaks were identified in the DTH site (right inflamed eyelid). A selection of representative major peaks is given in Fig. 2. By contrast, only nine minor peaks could be identified in the left eyelid (data not shown), indicating that the profusion of T cell clones at the DTH site was linked to the local immune response. Accordingly, the ensemble of peaks/clones constitutes a reference against which the dynamics of the T cell repertoire in peripheral blood pre- and post-BCG inoculation may be scored. A checkerboard representation of 19 infiltrating T cell clones present at the DTH site as a function of the serial PBMC samples and splenic mononuclear cells (SMC) is shown in Fig. 3. All were found in the periphery at some time while all but one clone were present in SMCs at death.

The clones could be divided into two groups based on their appearance in blood samples. The first comprises clones generally detected throughout the course of the experiment which were, importantly, present before initial BCG inoculation. The second group consisted of T cell clones

Fig. 2 A typical collection of T cell clones infiltrating the DTH reaction site. The Y-axis shows fluorescent intensity in arbitrary units. The X-axis shows the length of the CDR3 regions. Major peaks (asterisk) are defined as having a peak area of >3000 while minor peaks are between 600 and 3000.



that appeared in blood by day 21 after BCG1. For many clones in both groups, expansion was observed around days 7–10 post BCG2, while most clones were present in peripheral blood and in the spleen at the time of death, two days after BCG3.

In an attempt to define the subset of these T cell clones, splenocytes were separated into CD8+ and CD8- fractions using magnetic beads coated with CD8 specific mAb. Both CD8+ and CD8- (i.e., CD4+) T cell clones were found within the first group whereas the second harbored only CD4+ clones. Due to limited material, a number of clones could not be clearly identified as being CD8+/- for both groups (Fig. 3 legend). In keeping with what is known about T cell infiltration into DTH sites¹⁷, group 2 clones are probably BCG-specific CD4 T cells. Group 1 T cell clones cannot be BCG-specific as they pre-dated initial BCG inoculation. Furthermore three of five clones corresponded to CD8 T cells. Their presence in the right eyelid and their expansion in PBMCs at 7–10 days post BCG2 beg two questions: how were they recruited to the DTH site; and what was the stimulus for local and systemic amplification? If, apart from PPD, SIV was also present at the DTH site, then the recruitment of SIV-specific CD4+ and CD8+ cells would be anticipated.

SIV infiltration of DTH site

The V1 and V2 hypervariable regions of the SIV *env* gene were PCR amplified from total DNA extracted from either the DTH site (right eyelid) or the normal left eyelid as a control. SIV proviral DNA was detected in the right eyelid yet absent from the left eyelid even after nested PCR (Fig. 4). As a positive amplification control, a fragment of comparable length corresponding to the CD3 γ chain gene was amplified, and no difference was noted between left and right eyelid samples. The amplified SIV DNA infiltrating the DTH site was cloned and sequenced.

Of the 34 recombinants sequenced, 33 belonged to a variant characterized by an 18 bp duplication in V1 (Fig. 5a). (Sequences bearing these motifs are henceforth referred to as "eyelid" variants.) A SplitsTree2 phylogenetic analysis^{23,24} revealed two clus-

TCR	size bp	CD4/8	BCG1									BCG2						BCG3			
			-21	-11	-7	-3	0	+3	+6	+10	+21	R-3	R0	R+3	R+7	R+10	R+21	R+25	R+27	SMC	Eyelid
Group 1																					
Vβ3-Jβ1.6	211	ND																			
Vβ3-Jβ2.3	155	ND																			
Vβ3-Jβ2.3	157	ND																			
Vβ3-Jβ2.5	160	ND																			
Vβ3-Jβ2.5	162	ND																			
Vβ3-Jβ2.6	190	ND																			
Vβ3-Jβ2.6	195	ND																			
Vβ4-Jβ2.7	219	CD4																			
Vβ5-Jβ1.6	170	CD4																			
Vβ5-Jβ2.4	135	CD8																			
Vβ5-Jβ2.7	144	CD8																			
Vβ20-Jβ1.6	207	CD8																			
Group 2																					
Vβ3-Jβ2.7	183	ND																			
Vβ3-Jβ2.7	187	CD4																			
Vβ5-Jβ1.5	134	ND																			
Vβ7-Jβ1.5	174	CD4																			
Vβ7-Jβ2.7	184	ND																			
Vβ7-Jβ2.7	187	CD4																			
Vβ20-Jβ2.7	185	CD4																			

ters based on eyelid sequences 27 and 32, the latter being closer to the SIV_{mac251} origin (Fig. 5b). It is possible to test the assumption that sequence 32 represented a founder sequence with all others derived from it. In view of an HIV/SIV base substitution rate of 2.5×10^{-5} per base per cycle²³⁻²⁵, a replication span of between 10–24 hours¹⁴ and two days between BCG3 and sacrifice, approximately 0.3–0.6 substitutions would be anticipated among a collection of 33 such SIV V1V2 sequences (see Fig. 5 legend). The observed minimum number of point substitutions scored for these sequences was 12. Even if both sequences (27 and 32) were considered as founder sequences, four and six substitutions could be scored—far greater than the expected values. In short there is too much diversity to support the above hypothesis, and the sequences must either reflect multiple encounters between BCG activated CD4 T cells and circulating blood borne virus or result from the recruitment of multiple BCG-specific T cells which were previously infected by eyelid variants.

Temporal dynamics of eyelid sequences

The spatial variation of SIV and the low titers of infectious virus/PBMCs as a function of total virus/provirus load, preclude a reliable comparison of SIV quasispecies derived from the DTH site and peripheral blood. However, the temporal structure of SIV quasispecies and their correlation with BCG inoculation, as well as sampling multiple lymphoid organs, may shed light on the source of the eyelid sequences. Accordingly, SIV_{mac251} V1V2 DNA was amplified from total DNA derived from the sequential PBMC samples, cloned and approximately 20 clones per sample sequenced. All samples were positive for SIV DNA. The proportion of eyelid sequences in each sample is shown in Fig. 6a. They first appeared seven days after BCG2, peaked at ten days and declined thereafter. Interestingly, the presence of the eyelid sequence in blood follows the same kinetics as the TCR profiles of DTH-T cell clones, suggesting a link to the anamnestic BCG response.

Eyelid sequences were found in pooled SMCs (Fig. 6b), microdissected splenic white pulps (Fig. 6b) and in four out of five

Fig. 3 Checkerboard representation of DTH T cell clones over time in PBMCs and SMCs. The clone names and sizes in base pairs are shown on the left. Clones present in CD8+ and absent in the CD8- fractionated splenocytes were considered as CD8, while clones amplified in the CD8- and absent from the CD8+ fractionated splenocytes were considered as CD4. ND, not determined due to insufficient cells or a fluorescent intensity below 600. Clones with a peak area of 0–600 are left white; those from 600–3000 are grey; and those >3000 are black. On the far right, TCR profiles for the same clones present in SMCs and the right eyelid (DTH site) are shown.

lymph nodes (Fig. 6c) at the time of death, representing 9.6% of a total collection of 354 SIV sequences analyzed at death. As BCG injections were performed intravenously, some of those immune reaction sites must have been activated in response to BCG3 (i.e. splenic white pulps and lymph node germinal centers). Whether the SIV DNA is derived from splenic mononuclear cells, microdissected splenic white pulps or draining or distal lymph nodes, nothing approaching a frequency of 97% (33/34) of eyelid sequences obtained at the DTH site was observed. It is therefore improbable that the eyelid sequences detected at the DTH site represent chance encounters of circulating virus with anti-BCG activated CD4 T cells or trapping of PBMCs harboring SIV proviruses. Rather, our results support a tight association between BCG-activation of latently infected CD4 T cells and subsequent replication of SIV genomes bearing the SIV eyelid motif.

Although eyelid sequences were first detectable in the periphery at day seven after BCG2 (Fig. 6a), SIV variants bearing some of its traits could be found in peripheral blood samples immediately preceding BCG2, notably sequence R-3.8 (Fig. 7). Given the quasispecies nature of SIV and finite sequencing (approximately 20 clones per sample) this finding suggests that the eyelid sequence was already present at the time of BCG2, its frequency in

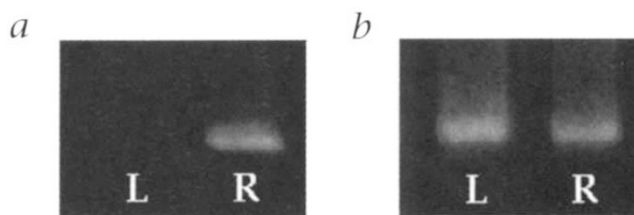


Fig. 4 a, Nested PCR amplification of SIV env V1V2 region and b, CD3 γ chain gene segment from Mm247 eyelids two days post-BCG3. The skin patches were of comparable sizes. Cells were extracted from the tissue by mechanical disruption followed by collagenase treatment after which total DNA was phenol extracted. One microgram of DNA was used for each amplification.

ARTICLES

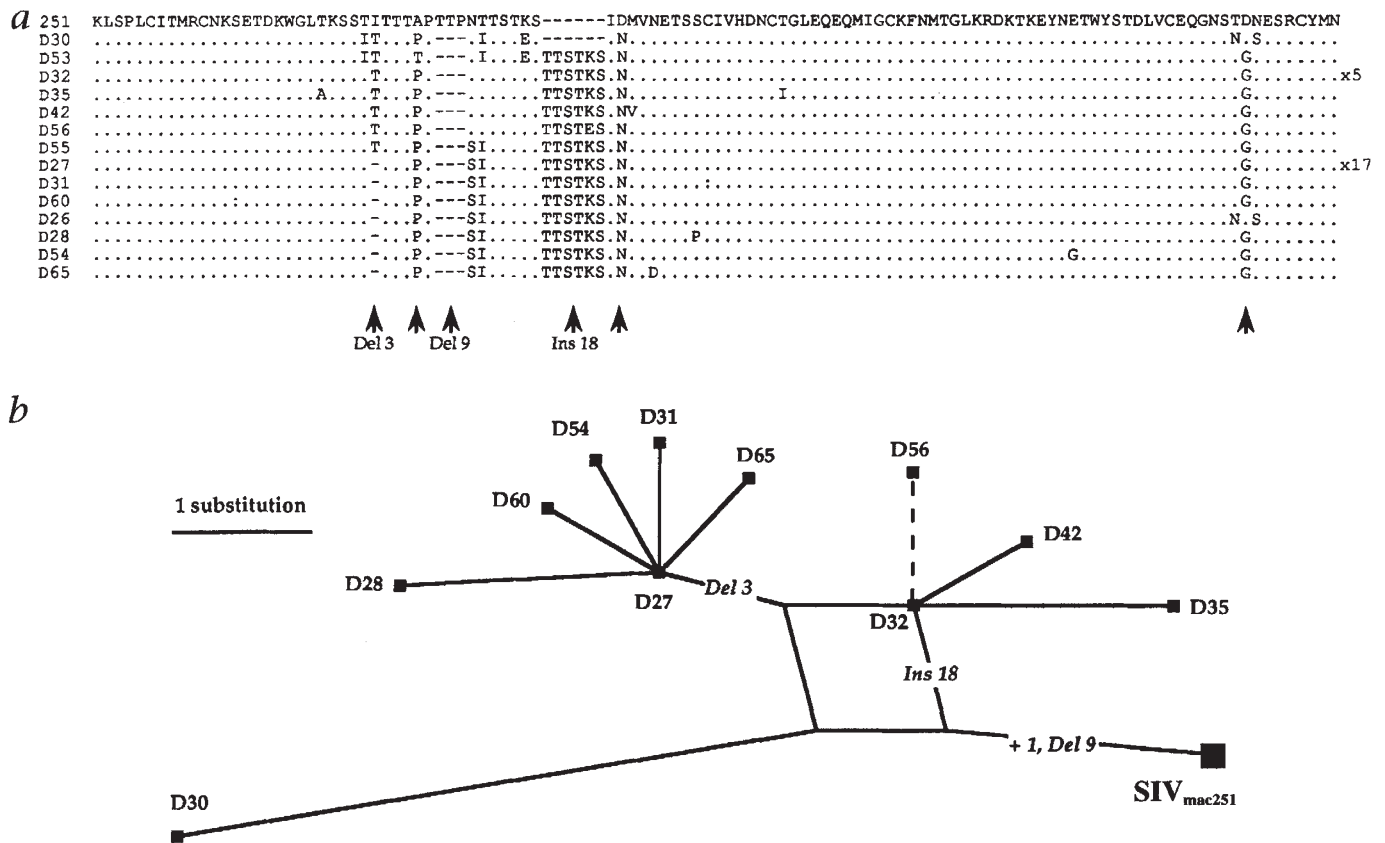


Fig. 5 Phylogenetic relationship of DTH derived SIV V1V2 sequences. **a**, Sequence alignment to that of the SIV_{mac251} reference (input) which dominated in all of the quasispecies found at 18 weeks post infection. Only sequence differences are shown, colons represent synonymous substitutions, gaps (-) being introduced to maximize sequence homology. All but sequence D30 carried a number of motifs (arrowheads) most notable of which were a 18 bp duplication and a 9 bp deletion. **b**, Phylogenetic relationship of SIV sequences. With respect to D32, D56 contained a single substitution within the 18 bp duplication which was eliminated from the

calculation. However its relationship to eyelid sequences is shown by the dotted line. A total of 20 substitutions (18 transitions and 2 transversions) were discerned. Were this number to be randomly distributed throughout the SIV_{mac251} reference sequence, the number of expected non-synonymous and synonymous would be 14.4 and 5.6 respectively. This distribution is not significantly different ($\chi^2 = 0.08$, 1 degree) compared to the 15 non-synonymous and 5 synonymous observed indicating that these substitutions were essentially unconstrained. In this respect this observation confirms the findings of a previous study¹⁴.

the periphery (particularly R+7 and R+10, Fig. 6) being amplified by BCG inoculation from between 5% and 35%.

Discussion

The kinetics of Mm247 immune responses were typical for primary and secondary human immune responses to BCG, which are detected approximately 21 and 7–10 days post immunization respectively^{19,20,26}. The emergence of group 2 CD4+ T cell clones in peripheral blood around 7–10 days, coincident with a maximum in the proportion of SIV eyelid sequences, suggests a link between activation of BCG-specific T cells and SIV eyelid variant replication. The question becomes how SIV arrived at the DTH site? The present data indicates that it was via recruitment of infected cells rather than infection *in situ* by circulating virus.

The distinctive sequence motifs of the eyelid sequence, most notably the 18 bp duplication, were fortuitous in that they constituted a genetic marker. The wealth of SIV sequence data coupled to the dynamics of TCR profiles allowed reconstruction of a plausible sequence of events. Presumably during the primary immune response to BCG, the eyelid ancestor (Fig. 7) became associated with a BCG-specific T cell clone. After BCG2 inoculation the clone was re-activated and proliferated in the secondary lymphoid organs, resulting in selective amplification of the eyelid variant over and above other SIV variants. At the same sites (splenic white pulps, lymph nodes germinal centers) other BCG-specific T cell clones were proliferating permitting the spread of the eyelid variant yet maintaining its association with anti-BCG immune response. The outpouring of the eyelid variant into the periphery and subsequent decline is typical of a secondary BCG immune response which is maximal around 7 days post inoculation^{18,26}. As Mm247 was killed two days post BCG3, it is perhaps not surprising that the proportion of eyelid sequences in the periphery was as low as 5% as BCG specific T cells would be sequestered in the lymphoid organs and the DTH site.

Evidence for dissemination also came from *in vitro* experiments. CD8- mononuclear cells, purified from the right maxillary lymph node (LN3) draining the right eyelid and the corresponding left node (LN4), were cultured in the presence of IL-2 in order to stimulate *in vivo* activated cells. After five hours, the viral quasispecies present in the culture supernatants were analyzed by RT-PCR. Interestingly, eyelid viruses were almost exclusively recovered from LN3, while absent from LN4 culture supernatant (data not shown), indicating that this variant was actively replicating in the lymphoid structure draining the DTH

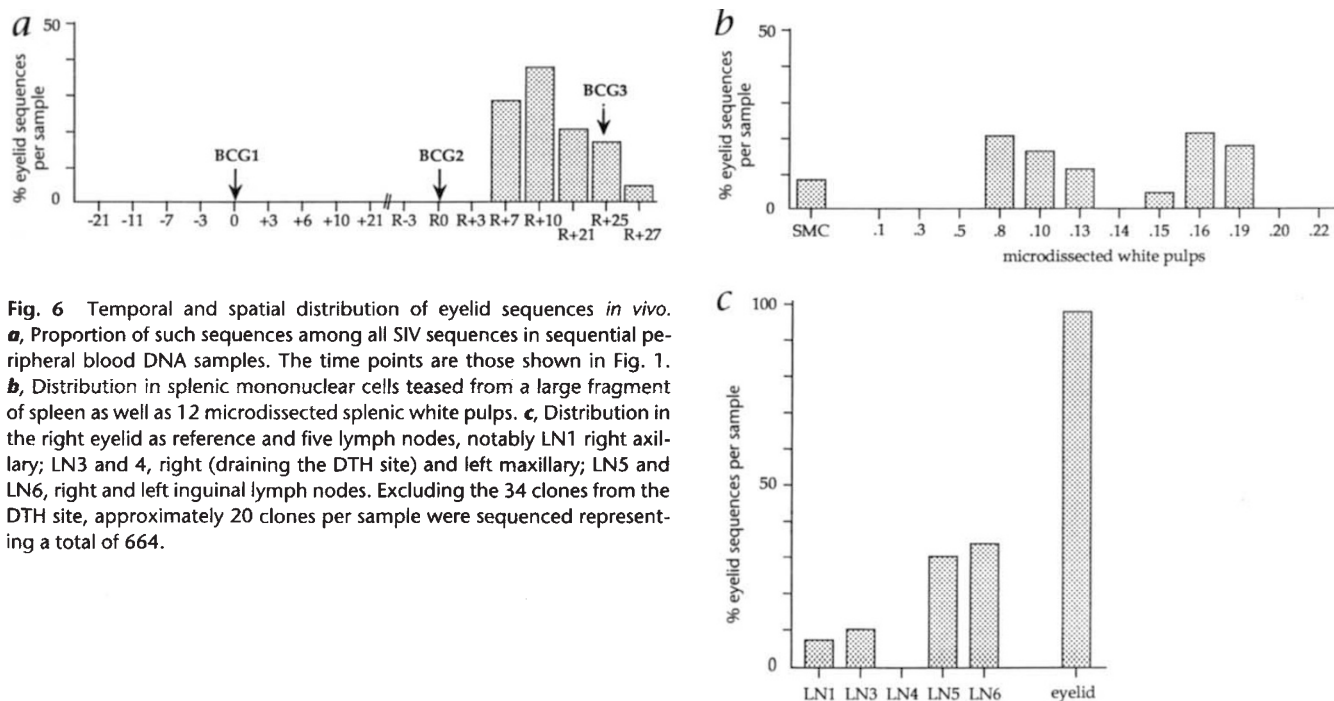


Fig. 6 Temporal and spatial distribution of eyelid sequences *in vivo*. **a**, Proportion of such sequences among all SIV sequences in sequential peripheral blood DNA samples. The time points are those shown in Fig. 1. **b**, Distribution in splenic mononuclear cells teased from a large fragment of spleen as well as 12 microdissected splenic white pulps. **c**, Distribution in the right eyelid as reference and five lymph nodes, notably LN1 right axillary; LN3 and 4, right (draining the DTH site) and left maxillary; LN5 and LN6, right and left inguinal lymph nodes. Excluding the 34 clones from the DTH site, approximately 20 clones per sample were sequenced representing a total of 664.

site. Hence localized *in vivo* BCG stimulation leads to dissemination of SIV. RT-PCR was also performed on total RNA isolated from lymph node (LN5, right inguinal) mononuclear cells. About 50% of the SIV clones sequenced harbored the eyelid motif confirming that these genomes were replicating at the time of death (data not shown).

Group 1 T cell clones could not be BCG-specific, being present in the periphery before BCG1. Like BCG specific clones, these T cell clones were expanded in the periphery at days seven and ten post-BCG2. One explanation for their infiltration into the DTH site is that they are SIV-specific clones recruited by infected BCG-specific clones. The presence of these CD8+ T cell clones in a majority of splenic white pulps (data not shown) is reminiscent of the observation of infiltrating anti-HIV CTLs in human splenic white pulps¹². This co-expansion of BCG-specific and SIV-specific clones is concordant with an immunopathological model of SIV infection. Indeed, as T cells are activated by their specific antigen, they either become targets for SIV infection or become centers for viral production in the case of those harboring latent provirus. SIV replication ensues with the inevitable generation and accumulation of mutants. At the same time, these infected T cells become targets for destruction by SIV specific CTLs. However, the elimination of the BCG-specific CD4 T cell population by anti-SIV immune responses is partial, as three BCG inoculations did not prevent a classic DTH response. It would be interesting to evaluate how many rounds of stimulation are necessary to completely eliminate a memory T cell response to a given antigen.

The present data demonstrate, *in vivo*, the juxtaposition of antigen, SIV replication and immune responses, that was hitherto inferred⁹. The remarkable short term stability of plasma viremia presumably reflects immune system activation by omnipresent environmental microbes and antigens. Stimulation with recall antigens *ex vivo*^{10,27} or vaccinia virus superinfection in the case of simian immunodeficiency virus (SIV) infected monkeys²⁸ results in HIV/SIV proliferation. Indeed, HIV is isolated following PHA activation of mononuclear cells. The former ex-

amples emphasize the point that HIV infection can be propagated by infection of recently activated T cells while the latter underlines the importance of latently HIV-infected T cells in sustaining viremia. Clearly, the current data represents a single case study and further work is required to develop the notion that antigen recruitment of specific T cells drives SIV replication.

Microbial replication is held in check by both non-specific and antigen specific immunity. The latter involves activation and proliferation of CD4 T cells which, in the case of HIV/SIV infection, become its prey. The outcome of this vicious circle clearly depends upon the relative kinetics of viral replication and immune responses which, given the polymorphism of outbred populations, are probably variable. The association of AIDS with opportunistic infections is well established and appears to be deleterious²⁹⁻³¹. By this logic drug treatment of opportunistic infections directly reduces viral load³². Vaccination of HIV infected patients must be used with care as any stimulation of the immune system will not only lead to a transient increase of viremia⁵⁻¹¹ but, as shown here, may also lead to the appearance and dissemination of new HIV variants. However, given the widespread interest in reservoirs of infection³³⁻³⁶ and their importance in sustaining proviral load in the face of highly active anti-retroviral therapy, it might be possible to exploit antigen stimulation as a means of depleting them, limiting further the risk of drug resistant variants.

Methods

Macaques, immunization protocol and samples. Three macaques were infected with the SIVmac251 strain. Details of the infection and immunization protocols are shown in Fig. 1. Non-recombinant BCG (Pasteur 1173) was used with a titer of 1.7×10^8 viable cfu/ml with 59% viability. It was sonicated for 4×15 seconds at room temperature and once for 15 seconds in warm water. All inocula were 1 ml. Two or three days after the third BCG boost, the animals were killed. Five lymph nodes (LN1, right axillary; LN3 and LN4, right and left maxillary; LN5 and LN6, right and left inguinal) and the spleen were collected. Both eyelids were also dissected and frozen. White pulps were microdissected from the spleen and DNA was extracted as described⁹.

ARTICLES

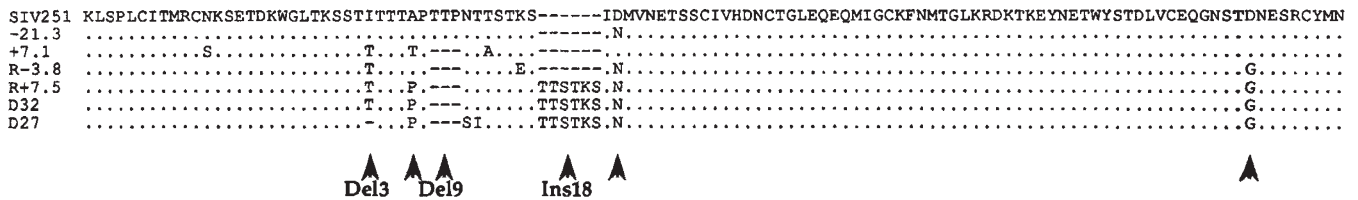


Fig. 7 Precursors to the "eyelid" sequences D32 and D27 in peripheral blood samples. Sequences are represented as in Fig. 5. They were among sets derived from samples -21, +7, R-3 and R+7 (Fig. 1) as reflected by the numbers/letters before the decimal, the number after the decimal refers to

the individual sequence. The defining traits are indicated by arrowheads. They are steadily accumulated over time. Given the quasispecies nature of SIV and the limitations of sampling the eyelid sequence R+7.5 was in all probability present, with low frequencies, in samples R-3 and R0.

PCR. Amplification of SIV_{mac} env V1V2 and TCRBV sequences were performed as previously described, albeit adapted to the macaque TCRBV loci^{12,37}, on 1 µg of each DNA or on microdissected splenic white pulps. A linear amplification of TCRBV rearrangements, CD3γ and SIV V1V2 was first realized with a mixture of four primers (SIVout3, CD3-100, jβ1.6-100 and jβ2.7-100). All PCR were performed according to the XL PCR conditions³⁸ and consisted of a denaturation step at 95 °C for 5 min., followed by 100 cycles (95 °C for 30 sec., 55 °C for 30 sec., 72 °C for 10 min.), in a thermal cycler with Ampliwax (Roche). Each linearly amplified product was then used as a template for specific amplification using either SIV-specific primers (SIVout5 and SIVout3) or a single TCRBV primer²¹ in combination with the 13 TCRBJ-30 primers or CD3γ-specific primers (CD3A and CD3B). PCR reactions were carried out for 35 cycles as above except 72 °C for 5 min., still using XL PCR and hot start conditions. For SIV, nested PCR was also performed when insufficient DNA was available for cloning using the SIVin3 and SIVin5 primers. For the cloning of specific TCR rearrangements, DNA from the right eyelid was used as the template and amplification was performed using the desired combination of TCRBV and TCRBJ primers, under the same conditions as above for 35 cycles. Cloning of blunt-end PCR fragments and sequencing was as described¹².

Run-offs. To analyze CDR3 length polymorphism, linear amplification of TCR rearrangements was performed with TCRBJ-specific primers coupled with the Fam fluorophore via a 5'-amino link II group as recommended (Applied Biosystems). The run-off reaction was performed in a volume of 20 µl using 10 µl of the amplified product as a template and the Stoffel fragment of Taq polymerase (Perkin-Elmer-Cetus) with the same conditions as described above. The products were linearly amplified for 20 cycles (95 °C for 30 sec., 60 °C for 30 sec., 72 °C for 2 min.). A mixture consisting of a quarter of the amplified products and molecular weight markers coupled to the Rox fluorophore (Applied Biosystems) in formamide were separated on a 6% acrylamide 7M urea gel on a ABI 373 DNA Sequencer (Applied Biosystems) and data was collected and analyzed using the GeneScan Data Collection and Analysis software (Applied Biosystems).

Primers. The SIVenvV1V2 primers were specific for the mac₂₅₁ sequence. SIVout5 GAGGACGTATGGCAACTCTTTGAG, SIVin5 TTGAGACCTCAAT-AAAGCCTTGTG, SIVin3 CAAGATTCTTGGATAACAGAAGTG, SIVout3 TAAG-CAAAGCATAACCTGGAGGTG. Rhesus monkey TCRBV specific oligonucleotides are available^{21,22} while primers mapping 3' to the TCRBJ regions were chosen based on the *M. mulatta* TCRBJ loci³⁷; Sjβ1.1-30 TGGACC-CACCTTTCCCTATGACGG, Sjβ1.2-30 TCTTTGACATTTCCAGGACAGAG, Sjβ1.3-30 TTAACCTAAGCACTGGAGACAAG, Sjβ1.4-30 CAGTGTCTACC-CTCCCCAAGGGG, Sjβ1.5-30 ATCCTCTCACCAGTGTGGAAGG, Sjβ1.6-30 CTTCACGCAACAGATAATTGCGG, Sjβ1.6-100 TGACCCTGAC-CTCCATTTCATACATC, Sjβ2.1-30 GGTTCTGGGGTCGCCAGGCTGGG, Sjβ2.2-30 AGCACAGCCCCTCTCGGAGTGGGG, Sjβ2.3-30 AGCA-CAAAAATGGCCCTGCTATG, Sjβ2.4-30 AACCCGACGCCGTCTCC-CCAGG, Sjβ2.5-30 TCCCACAAAACCGGACCCAAG, Sjβ2.6-30 CCTAGCACAGGGGGGACAGG, Sjβ2.7-30 GAGCGGGGAGGTGACG-CTGCAGAG, Sjβ2.7-100 TGTCTTCCCAGGAGCGGGGAGGTG.

Those marked by the Fam fluorophore were coupled at the 5' end by an aminolink II; Sjβ1.1fluo ACTTTTCCCTGTGACGGATCTGCAA, Sjβ1.2fluo CCCTCATCGCACCCCTCTAGAGACC, Sjβ1.3fluo AGTGTCCAGCC-TTGACTTACTCAC, Sjβ1.4fluo CCTTATAACACACTATCCCAAAG,

Sjβ1.5fluo TACCACCTGATTCTGCCAATTAC, Sjβ1.6fluo GCAACAG-CTAATTGCTTTCAAACCC, Sjβ2.1fluo GCCCTCCCTCTCTCCACCTGGAG, Sjβ2.2fluo CCGCCCTCTCGGAGCGCTCCGGAG, Sjβ2.3fluo TTACCGAGC-ACCTCAGCCGGT, Sjβ2.4fluo AGTCCCCCGGCCCCAGCTTA, Sjβ2.5fluo CCCCCTCACCAGCAGCAGGAG, Sjβ2.6fluo CACCCGGA-CCCCCGCTCCGGT, Sjβ2.7fluo GACCCAGGGGCTGGAGGTGGAGAG. Those for CD3γ chain amplification were: CD3-100 GTCCACTGCTAGCCC-CCAGCTCGTAAGTA, CD3A GCCTGGCTGTCTCATCTGGCTATC, CD3B TGGCCTATGCCCTTTTGGGCTGCATC.

Phylogenetic studies. The phylogenetic relationship of SIV sequences was determined by the SplitsTree2 program²³ and <ftp://ftp.uni-bielefeld.de/pub/math/splits/splitstree2> or <http://www.bibiserv.techfak.uni-bielefeld.de/splits>. Gaps were removed leaving 320 characters, a Hamming distance matrix was used and bootstrapped 1000 times. The values for simple branches involving one and two mutations were >60% and >86% respectively. The low value for single mutations is to be expected. Ambiguously linked sequences (D26 and D53 which could be recombinants) were excluded. Thereafter 100% of data was used to construct the tree.

ELISA. ELISA plates were coated with Tuberculin PPD (Central Veterinary Laboratory, Weybridge, England) at 1 mg/ml. After saturation with BSA (3%), incubation with serial dilution of the macaques sera, anti-PPD immunoglobulins were revealed by alkaline phosphatase conjugated anti-monkey IgG (Sigma Immunochemicals).

Acknowledgements

We thank Eric Pelletier and Sven Henrichwark for help with sequencing and Marina Gheorghiu for providing reagents for the ELISA and mouse control sera. This work was supported by grants from the Institut Pasteur, l'Agence Nationale pour la Recherche sur le SIDA (ANRS), and grants AI-20729 from the NIH. S.G. was supported by fellowships from the ANRS and NHRDP (Canada). I.S. was supported by a fellowship from the ANRS.

RECEIVED 8 JANUARY; ACCEPTED 25 FEBRUARY 1998

- Mclroy, D., et al. Infection frequency of dendritic cells and CD4+ T lymphocytes in spleens of human immunodeficiency virus-positive patients. *J. Virol.* **69**, 4737-4745 (1995).
- Schnittman, S.M. et al. Preferential infection of CD4+ memory T cells by human immunodeficiency virus type 1: evidence for a role in the selective T-cell functional defects observed in infected individuals. *Proc. Natl. Acad. Sci. USA* **87**, 6058-62 (1990).
- Zack, J.A., et al. HIV-1 entry into quiescent primary lymphocytes: molecular analysis reveals a labile, latent viral structure. *Cell* **61**, 213-222 (1990).
- Gaynor, R.B. Regulation of HIV-1 gene expression by the transactivator protein. *Curr. Top. Microbiol. Immunol.* **193**, 51-77 (1995).
- Claydon, E.J., Bennett, J., Gor, D. & Forster, S.M. Transient elevation of serum HIV-1 antigen levels associated with intercurrent infection. *AIDS* **5**, 113-114 (1991).
- Fultz, P.N., Gluckman, J.C., Muchmore, E. & Girard, M. Transient increases in numbers of infectious cells in an HIV-1 infected chimpanzee following immune activation. *AIDS Res. Hum. Retroviruses* **8**, 313-317 (1992).
- Brichacek, B., Swindells, S., Janoff, E.N., Pirruccello, S. & Stevenson, M. Increased plasma human immunodeficiency virus type 1 burden following antigenic challenge with pneumococcal vaccine. *J. Infect. Dis.* **174**, 1191-9 (1996).
- Ho, D.D. HIV-1 viremia and influenza. *Lancet* **339**, 1549 (1992).
- O'Brien, W.A. et al. Human immunodeficiency virus type 1 replication can be in-

- creased in peripheral blood of seropositive patients after influenza vaccination. *Blood* **86**, 1082–1089 (1995).
10. Stanley, S.K. *et al.* Effect of immunization with a common recall antigen on viral expression in patients infected with human immunodeficiency virus type 1. *N. Engl. J. Med.* **334**, 122–1230 (1996).
 11. Staprans, S.I. *et al.* Activation of virus replication after vaccination of HIV-1 infected individuals. *J. Exp. Med.* **182**, 1727–1737 (1995).
 12. Cheynier, R. *et al.* HIV and T cell expansion in splenic white pulps is accompanied by infiltration of HIV-specific cytotoxic T lymphocytes. *Cell* **78**, 373–387 (1994).
 13. Levy, J.A. The value of primate models for studying human immunodeficiency virus pathogenesis. *J. Med. Primatol.* **25**, 163–74 (1996).
 14. Pelletier, E., Saurin, W., Cheynier, R., Letvin, N.L. & Wain-Hobson, S. The tempo and mode of SIV quasispecies development in vivo calls for massive viral replication and clearance. *Virology* **208**, 644–652 (1995).
 15. Wain-Hobson, S. Viral burden and AIDS. *Nature* **366**, 22 (1993).
 16. Burns, D.P.W. & Desrosiers, R.C. Selection of genetic variants of simian immunodeficiency virus in persistently infected rhesus monkeys. *J. Virol.* **65**, 1843–1854 (1991).
 17. Kuramoto, Y., Sekita, Y. & Tagami, H. Histoanalytical study of the cellular infiltrate in the tuberculin reaction. *Clin. Exp. Dermatol.* **18**, 111–118 (1993).
 18. Bleavins, M.R. & de la Iglesia, F.A. Cynomolgous monkeys (*Macaca fascicularis*) in preclinical immune function safety testing: development of a delayed-type hypersensitivity procedure. *Toxicology* **95**, 103–112 (1995).
 19. Pilkington, C., Costello, A.M., Rook, G.A. & Stanford, J.L. Development of IgG responses to mycobacterial antigens. *Arch. Dis. Child.* **69**, 644–9 (1993).
 20. Rota, S., Beyazova, U., Karsligil, T. & Cevheroglu, C. Humoral immune response against antigen 60 in BCG-vaccinated infants. *Eur. J. Epidemiol.* **10**, 713–8 (1994).
 21. Chen, Z.W., Yamamoto, H., Watkins, D.I., Levinson, G. & Letvin, N.L. Predominant use of a T-cell receptor V β gene family in simian immunodeficiency virus gag-specific cytotoxic T lymphocytes in a rhesus monkey. *J. Virol.* **66**, 3913–3917 (1992).
 22. Chen, Z.W., Kou, Z.-C., Shen, L., Reimann, K.A. & Letvin, N.L. Conserved T-cell receptor repertoire in simian immunodeficiency virus-infected rhesus monkeys. *J. Immunol.* **151**, 2177–2187 (1993).
 23. Bandelt, H.J. & Dress, A.W.M. Split decomposition: a new and useful approach to phylogenetic analysis of distance data. *Mol. Phylogenet. Evol.* **1**, 242–252 (1992).
 24. Dopazo, J., Dress, A.W.M. & von Haeseler, A. Split decomposition: a new technique to analyse viral evolution. *Proc. Natl. Acad. Sci. USA* **90**, 10320–10324 (1993).
 25. Mansky, L.M. & Temin, H.M. Lower in vivo mutation rate of human immunodeficiency virus type 1 than that predicted from the fidelity of purified reverse transcriptase. *J. Virol.* **69**, 5087–5094 (1995).
 26. Ravn, P., Boesen, H., Pedersen, B.K. & Andersen, P. Human T cell responses induced by vaccination with *Mycobacterium bovis* Bacillus Calmette-Guérin. *J. Virol.* **158**, 1949–1955 (1997).
 27. Weissman, D., Barker, T.D. & Fauci, A.S. The efficiency of acute infection of CD4+ T cells is markedly enhanced in the setting of antigen-specific immune activation. *J. Exp. Med.* **183**, 687–692 (1996).
 28. Dittmer, U., Niblein, T., Meyerhans, A., Hunsmann, G. & Stahl-Henning, C. No re-activation of attenuated immunodeficiency viruses in macaques after vaccinia virus-induced immune activation. *J. Gen. Virol.* **78**, 2523–2528 (1997).
 29. Kreiss, J. *et al.* Association between cervical inflammation and cervical shedding of human immunodeficiency virus DNA. *J. Infect. Dis.* **170**, 1597–1601 (1994).
 30. Galai, N., Kalinkovich, A., Burstein, R., Vlahov, D. & Bentwich, Z. African HIV-1 subtype C and rate of progression among Ethiopian immigrants in Israel. *Lancet* **349**, 180–181 (1997).
 31. Bentwich, Z., Kalinkovich, A. & Weisman, Z. Immune activation is a dominant factor in the pathogenesis of African AIDS. *Immunol. Today* **16**, 187–191 (1995).
 32. Gerna, G. *et al.* Sharp drop in the prevalence of human cytomegalovirus leuko-DNAemia in HIV-infected patients following highly active antiretroviral therapy. *AIDS* **12**, 118–119 (1998).
 33. Chun, T.-W. *et al.* Quantitation of latent tissue reservoirs and total body viral load in HIV-1 infection. *Nature* **387**, 183–188 (1997).
 34. Finzi, D. *et al.* Identification of a reservoir for HIV-1 in patients on highly active antiretroviral therapy. *Science* **278**, 1295–1300 (1997).
 35. Perelson, A.S. *et al.* Decay characteristics of HIV-1 infected compartments and implications for eradication. *Nature* **387**, 188–191 (1997).
 36. Wong, J.K. *et al.* Recovery of replication-competent HIV despite prolonged suppression of plasma viremia. *Science* **278**, 1291–1295 (1997).
 37. Cheynier, R., Henrichwark, S. & Wain-Hobson, S. Sequence of the rhesus monkey T-cell receptor β chain diversity and joining loci. *Immunogenet.* **43**, 83–87 (1996).
 38. Cheng, S., Fockler, C., Barnes, W.M. & Higuchi, R. Effective amplification of long targets from cloned inserts and human genomic DNA. *Proc. Natl. Acad. Sci. USA* **91**, 5695–5699 (1994).